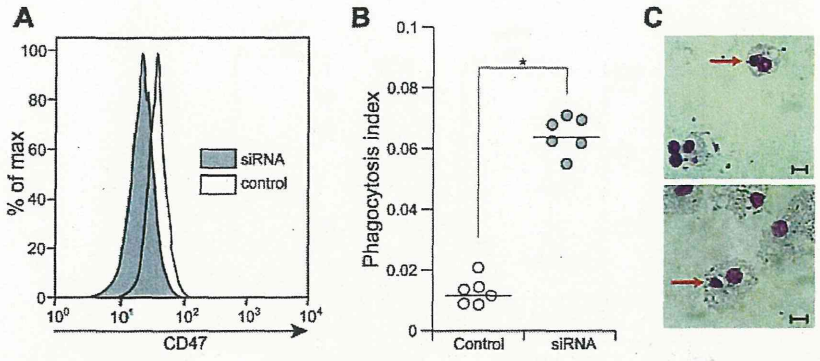

Figure 3. Knocking down CD47 in CD34$^+$CD38$^-$ cells induces their engulfment by macrophages. (A) Knockdown of CD47 expression in normal CD34$^+$CD38$^-$ cells by siRNA for human CD47. Treatment of CD34$^+$CD38$^-$ cells with siRNA for 48 hours induced 60% reduction of CD47 expression in these cells. (B) CD34$^+$CD38$^-$ cells treated with the siRNA for human CD47 showed accelerated engulfment by normal macrophages. Vertical axis shows the phagocytosis index (phagocytosis index = phagocytic macrophages/number of macrophages) and the bars show mean value. *$P < .01$ by conventional *t* test. (C) Engulfment of CD34$^+$CD38$^-$ cells treated with siRNA by normal macrophages (Giemsa staining). Scale bars indicate 10 μm.

Reduction of CD47 expression in HSCs in HLH patients results in engulfment of HSCs by macrophages

We also sought to investigate whether CD47 expression levels in target cells affect the efficiency of engulfment by macrophages. We first treated NB4, a human promyelocytic leukemia cell line, with 2 types of siRNAs targeting human CD47. siRNA1 showed a 72% reduction of CD47 expression in NB4 cells, whereas siRNA2 showed a 37% reduction (supplemental Figure 2A). We then quantitated the engulfment of macrophages by enumeration of the phagocytosis index (phagocytic macrophages/number of macrophages).[22,33,35,37] In the culture of these cells with normal macrophages, rare control NB4 cells were engulfed by macrophages, whereas NB4 cells treated with siRNA1 or siRNA2 showed 5- and 2.5-fold increases in the phagocytosis index, respectively, which illustrates the efficiency of engulfment by macrophages (supplemental Figure 2B). Therefore, the engulfment of NB4 evoked by CD47 suppression occurs in a dose-dependent manner.

We treated purified normal CD34$^+$CD38$^-$ HSCs with the siRNA1 for 24 hours and evaluated the phagocytosis index. As shown in Figure 3A, an approximately 30% reduction of the level of CD47 expression was observed in purified CD34$^+$CD38$^-$ cells treated with siRNA1. The CD34$^+$CD38$^-$ cells treated with siRNA1 became susceptible to phagocytosis, and showed 5.3-fold increase in the phagocytosis index compared with untreated CD34$^+$CD38$^-$ cells ($P < .01$). Therefore, the reduction of CD47 in CD34$^+$CD38$^-$ cells stimulates macrophages to engulf these cells.

We also investigated whether HSCs isolated from HLH patients are susceptible to phagocytosis by normal macrophages. We purified CD34$^+$CD38$^-$ HSCs and CD34$^+$CD38$^+$ progenitors from HLH patients (patients number 4, 16, and 22) and healthy controls and evaluated the phagocytosis index. As shown in Figure 4A, in all 3 HLH patient samples, CD34$^+$CD38$^-$ cells with a 40%-60% reduction of CD47 levels (Figure 2A) were actively engulfed by macrophages. In contrast, CD34$^+$CD38$^+$ cells of HLH patients showed a low phagocytic index, as was also observed in HSCs or progenitors in healthy controls (Figure 4A). Therefore, the efficiency of phagocytosis by macrophages is inversely correlated with the expression of CD47 of target cells even in human HLH samples, showing that a decrease of CD47 expression can induce engulfment of HSCs in HLH, at least in vitro.

Finally, we investigated whether HSCs were engulfed and reduced in number in HLH patients. We counted the number of CD34$^+$CD38$^-$ cells in BM from healthy controls and HLH patients (Figure 4B). The frequencies of CD34$^+$CD38$^-$ HSCs were significantly reduced in HLH BM (0.04% ± 0.02% of total nucleated cells) compared with those in normal adults (0.15% ± 0.09%). The number of nucleated cells in the BM was also reduced by approximately 50%. As a result, as shown in Figure 4B, the number of CD34$^+$CD38$^-$ cells in HLH patients was reduced down to only 23% of those in healthy adults. Although the number of CD34$^+$CD38$^+$ cells were also reduced in the HLH patients (approximately 42% of healthy adults), the reduction was more

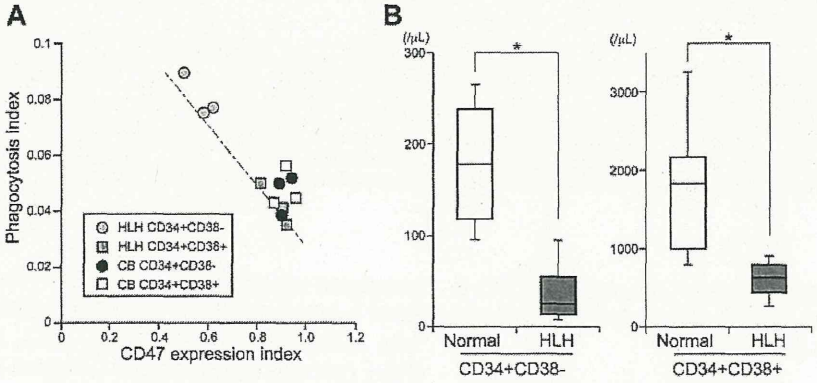

Figure 4. The CD34$^+$CD38$^-$ HSC fraction but not the progenitor population in HLH patients is sensitive to engulfment by macrophages. (A) Relationship between the level of CD47 expression and the phagocytosis index tested in vitro. CD34$^+$CD38$^-$ cells and CD34$^+$CD38$^+$ cells from 3 HLH patients (unique patient number [UPN] 4, 16, and 22) and healthy controls were cultured with activated macrophages. CD47 expression index represents the relative surface CD47 level calculated as the median CD47 levels of analyzed cells/those in normal blood mononuclear cells. The bar shows the regression line; the coefficient of correlation value was −0.91. (B) The number of CD34$^+$CD38$^-$ HSCs and CD34$^+$CD38$^-$ progenitor cells in the BM of HLH patients ($n = 14$) and healthy controls ($n = 6$) are shown in the box and whisker plot. HLH patients had significantly decreased numbers of HSC and progenitor populations, but the magnitude of suppression of HSCs was more profound. The bottom and top of the boxes are the 25th and 75th percentile values. The bands in the middle of the boxes represent the 50th percentile (median). Error bars show 1 SD differences above and below the mean of the data. *$P < .01$ by conventional *t* test.

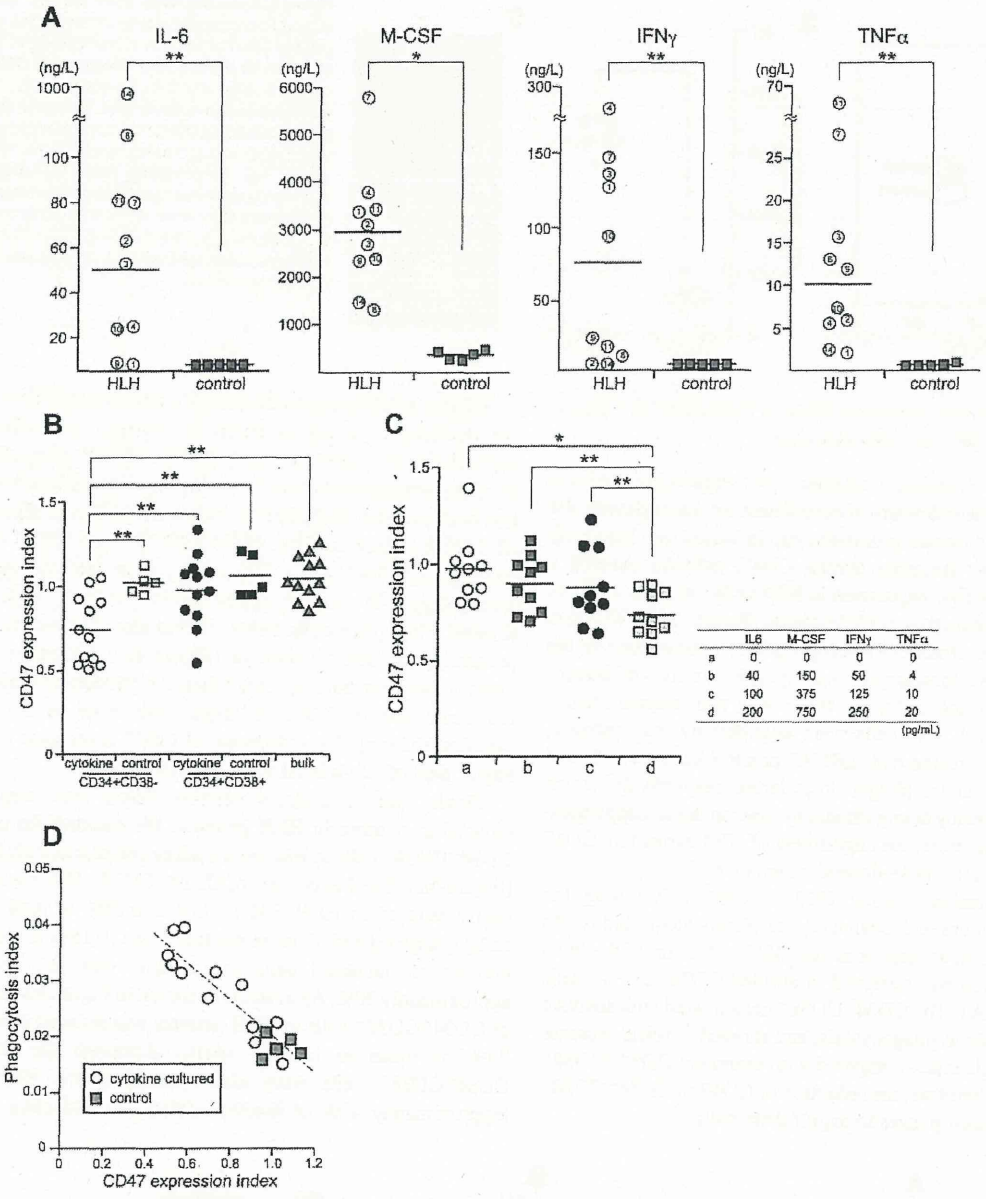

Figure 5. Inflammatory cytokines down-regulate CD47 specifically in CD34$^+$CD38$^-$ cells to induce engulfment by macrophages. (A) Serum levels of M-CSF, IL-6, TNF-α, and IFN-γ from in patients by ELISA. These cytokines were extremely high in HLH samples compared with healthy controls. *$P < .01$; **$P < .05$ by conventional *t* test. (B) Changes of CD47 expression levels in normal CD34$^+$CD38$^-$ HSCa and CD34$^+$CD38$^+$ progenitor cells in the presence of inflammatory cytokines. CD47 expression index represents the relative surface CD47 level calculated as median CD47 levels of analyzed cells/those in normal blood mononuclear cells. The HSC fraction, but not the progenitor fraction, showed down-regulated CD47 in response to cytokines. **$P < .05$ by conventional *t* test. (C) Suppression of CD47 in CD34$^+$CD38$^-$ cells by graded doses of inflammatory cytokines. The concentration of inflammatory cytokines is shown on the right. (D) Engulfment of HSCs by macrophages in response to reduction of CD47 expression by cytokines in vitro. The CD47 expression index was inversely correlated with phagocytosis index. The bar shows the regression line; the coefficient of correlation value was −0.89.

profound in the CD34$^+$CD38$^-$ fraction. The number of HSCs is reduced in the BM of HLH patient by phagocytosis that is evoked by HSC-specific reduction of CD47.

Inflammatory cytokines down-regulate CD47 expression and enhance the efficiency of engulfment of HSCs by macrophages

It has been shown that hypercytokinemia plays a critical role in the development of HLH. Consistent with previous results,[3] HLH patient sera contained high levels of inflammatory cytokines, including IL-6, M-CSF, IFN-γ, and TNF-α (Figure 5A). We investigated whether these cytokines can affect the expression of CD47 in hematopoietic cells. Lineage-depleted cord blood cells were cultured with M-CSF (750 pg/mL), IL-6 (200 pg/mL), IFN-γ (250 pg/mL), and TNF-α (20 pg/mL) for 24 hours, and CD47 expression was evaluated in stem, progenitor, and mature cell fractions. The concentrations of inflammatory cytokines were compared with those of HLH patient sera. CD47 expression was down-regulated specifically in CD34$^+$CD38$^-$ HSCs, whereas it did not change in CD34$^+$CD38$^+$ progenitors or unfractionated mature cells (Figure 5B). The down-regulation of

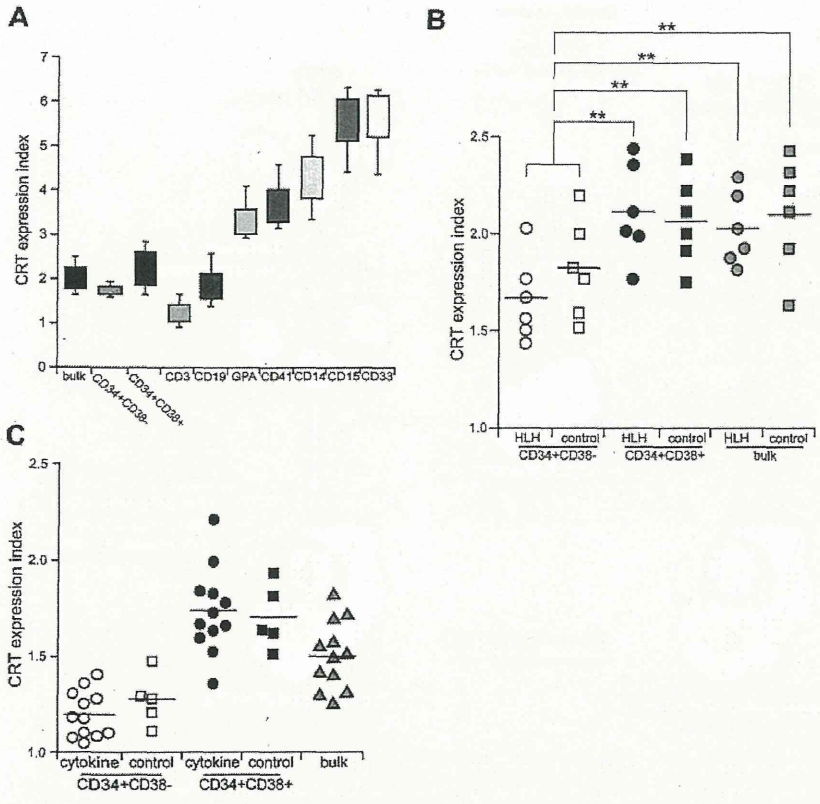

Figure 6. CRT is not involved in the engulfment of HSCs in HLH. (A) CRT expression in normal hematopoietic cells. CRT expression index represents the relative surface CRT level calculated as median CRT levels of analyzed cells/those in normal blood mononuclear cells. Error bars show 1 SD differences. (B) CRT expression in $CD34^+CD38^-$ HSCs, $CD34^+CD38^+$ progenitors, and unfractionated BM cells from HLH patients and healthy controls. The expression level of CRT was equivalent in HLH patients and healthy controls in all of these cell fractions. $^{**}P < .05$ by conventional *t* test. (C) The effect of cytokines on CRT expression. CRT expression was not changed irrespective of incubation with cytokines in any of these cell fractions. Bars show the mean values.

$CD47$ expression in $CD34^+CD38^-$ cells occurs in response to cytokines in a dose-dependent manner (Figure 5C). The cells treated with cytokines were further tested for phagocytosis assays. As shown in Figure 5D, the expression level of CD47 in $CD34^+CD38^-$ HSCs treated with inflammatory cytokines was inversely correlated with the phagocytosis index. These data suggest that inflammatory cytokines can down-regulate CD47 expression specifically in HSCs, inducing HSC-targeted engulfment by BM macrophages.

CRT, a dominant prophagocytic factor, is down-regulated in $CD34^+CD38^-$ HSCs in both HLH patients and healthy controls

CRT is the major prophagocytic factor expressed on the cell surface, which binds to lipoprotein-related protein on cell surface of macrophages and stimulates their phagocytic activities.[14] During apoptotic cell death, these cells are engulfed due to loss of CD47 expression and coordinated up-regulation of cell-surface CRT as thedominant prophagocytic signal.[38] We evaluated the expression level of CRT in stem, progenitor, and mature cell fractions in HLH patients. In the healthy BM, CRT was highly expressed in mature myeloid cells, but at a very low level in lymphoid cells. Erythroblasts and megakaryocytes expressed intermediate levels of CRT. Interestingly, the expression level of CRT was very low in immature hematopoietic cells, including $CD34^+CD38^-$ HSCs and $CD34^+CD38^+$ progenitor cell fractions (Figure 6A). $CD34^+CD38^-$ HSCs expressed even lower levels of CRT compared with those in $CD34^+CD38^+$ progenitors (Figure 6B). In HLH patients, the expression of CRT was comparable to that in healthy controls: The $CD34^+CD38^-$ HSC population expressed only a very low level of CRT (Figure 6B). We then cultured normal HSCs in the presence of inflammatory cytokines including M-CSF, IL-6, IFN-γ, and TNF-α for 24 hours, and the expression of CRT did not change in the HSC or progenitor populations (Figure 6C). Therefore, CRT is shut down at the HSC stage even in HLH patients, suggesting that the expression of CRT is not involved in engulfment of HSCs by macrophages.

Discussion

In HLH, cytopenia occurs in more than 80% of patients at disease presentation. The BM may present either hypocellularity or hypercellularity at the onset, but eventually becomes hypoplastic. This phenotype is thought to result mainly from suppression of hematopoiesis by elevated inflammatory cytokines such as TNF-α and IFN-γ and from engulfment of hematopoietic cells by BM macrophages.[39] The serum concentrations of these cytokine levels in HLH are usually quite higher than those with sepsis,[40] suggesting that these extremely high levels of cytokines should be critical in the pathogenesis of HLH. In the present study, we show that HLH patients have low numbers of HSCs, and that HSCs from HLH patients down-regulate CD47 and are prone to be engulfed by macrophages more actively than normal HSCs. We also show that inflammatory cytokines can down-regulate the expression of CD47 selectively in HSCs, resulting in a disruption of self-recognition based on the CD47-SIRPA system to induce engulfment of HSCs by macrophages. Based on these data, we propose that the disruption of the CD47-SIRPA system plays a primary role in the development of HLH.

Macrophages function to clear foreign, aged, or damaged cells via phagocytosis, and this process is regulated by the balance between antiphagocytic and prophagocytic signals. The primary

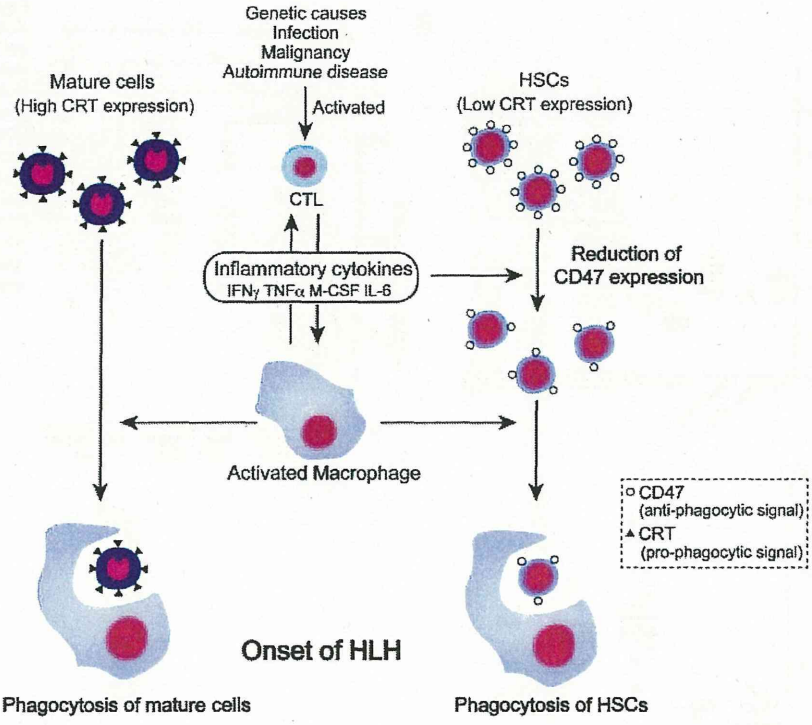

Figure 7. Pathogenesis of HLH based on antiphagocytic and prophagocytic signaling. In HLH, cytotoxic T lymphocytes are activated by genetic abnormality, infection, malignancy, and autoimmune disease, and then produce inflammatory cytokines and activate macrophages. Activated macrophages engulf mature cells such as RBCs, platelets, and granulocytes, which are susceptible to phagocytosis because of high expression of prophagocytic CRT. In contrast, inflammatory cytokines suppress hematopoiesis by their direct toxic effects and down-regulate CD47 expression on HSCs, resulting in a decreased threshold of antiphagocytic signals. Therefore, HSCs were engulfed by activated macrophages, causing the BM of HLH patients to become hypoplastic, thereby exacerbating pancytopenia.

antiphagocytic and prophagocytic signals for macrophages to engulf nonapoptotic cells are the CD47-SIRPA and the LPR-CRT systems, respectively.[14] Because in the present study, freshly isolated HSCs from HLH patients, but not from healthy controls, were engulfed by macrophages in vitro (Figure 4A), the balancing of this signaling should be altered in HLH.

Many polymorphisms have been detected in human SIRPA, especially in the ligand-binding IgV domain.[26] In the present study, however, HLH patients did not have any specific polymorphisms of SIRPA. In addition, we could not find differences in the level of SIRPA expression between normal and HLH BM cells. We conclude that neither polymorphisms of SIRPA nor the change of its expression levels are involved in the pathogenesis of HLH.

Conversely, the expression of CD47 was significantly down-regulated specifically in the HSC fraction in HLH patients, but was not changed in progenitors and other mature cells (Figure 2A-C). The expression level of CD47 in HLH HSCs was approximately 50% at the protein level compared with that in normal HSCs. This level of reduction readily induced macrophage activation in vitro (supplemental Figures 2 and 4A). BM HSCs in HLH patients were reduced in number, presumably by engulfment, but were functionally normal, at least in terms of colony-forming capabilities in vitro (supplemental Figure 1B). The down-regulation of CD47 in HLH HSCs might be induced by high levels of serum inflammatory cytokines such as IL-6, M-CSF, IFN-γ, and TNF-α, because incubation of normal HSCs, but not progenitors, with these cytokines induced down-regulation of CD47 in vitro in a dose-dependent manner (Figure 5B-C), and rendered normal HSCs susceptible to engulfment by macrophages (Figure 5D).

It remains unclear by what mechanism only the HSC fraction is sensitive to cytokines to down-regulate CD47. Interestingly, in contrast to the CD47 protein, the CD47 mRNA levels were normal in HSCs in all 5 HLH patients analyzed by quantitative real-time PCR assays (not shown), so the down-regulation of CD47 could occur at the posttranscriptional level. In a recent study, Junker et al examined miRNA profiles from active and inactive lesions in multiple sclerosis patients, and found out that miRNA-34a, miRNA-155 and miRNA-326, the targets of which include human CD47, were up-regulated in active sclerosis lesions.[41] These miRNAs reduce the expression of CD47 in brain-resident cells, promoting macrophages to engulf myelin. In the present study, we evaluated miRNA-34a, miRNA-155, and miRNA-326 expression in HSCs in HLH patients, but could not find any differences in the expression level of these miRNAs in HSCs from HLH patients and healthy controls (T.K., unpublished data, February 2010). Inflammatory cytokines did not induce the increased expression of these miRNAs (T.K., unpublished data, March 2010). It is critical to clarify the mechanism of CD47 down-regulation in the HSC fraction in future studies.

The expression of CRT on the cell surface is an important prophagocytic signal. When CRT binds to LPR on macrophages, LPR signaling immediately can stimulate macrophages to engulf the CRT-expressing cells.[14,15] This "eat me" signal could antagonize the "do not eat me" signal mediated by the CD47-SIRPA interaction.[42] Once apoptosis is initiated, CRT is up-regulated, phosphatidylserine is exposed to the cell surface, and CD47-SIRPA signaling is rendered ineffective, thereby permitting engulfment of target cells.[42] In contrast to CD47, which is ubiquitously expressed in normal hematopoietic cells from HSCs to mature cell stages (Figure 2A), CRT is expressed mainly in myeloerythroid cells, but only at a low level in immature $CD34^+CD38^-$ HSCs. Because recent studies have shown that macrophages are cellular components of HSC niches,[24] down-regulation of CRT might be required for HSCs to stay intact at the niche. In contrast, mature myeloerythroid cells might be primed to be prophagocytic via sustained CRT expression, which enables macrophages to engulf these cells on activation by, for example, cytokines.

Previous studies have shown that the CD47-SIRPA system is critical to engraftment and maintenance of HSCs in vivo. We have reported that the reason that human HSCs engraft efficiently in the

NOD mouse is that this strain has a polymorphic SIRPA capable of binding to human CD47.[26] Blocking the CD47-SIRPA interaction by antihuman CD47 Fc inhibited the engraftment of human HSCs in the NOD-SCID xenograft model. In fact, HSCs have contact with macrophages in the vascular or reticuloendothelial niche,[43,44] suggesting that self-recognition by macrophages could operate actively at the HSC niche. The impairment of antiphagocytic signals that involves HSCs specifically may be one of the primary mechanisms for the severe hypocellularity and pancytopenia seen in the BM of HLH patients.

A schematic of the proposed pathogenesis of HLH based on the results of the present study is provided in Figure 7. In HLH, elevated inflammatory cytokines activate macrophages. Mature blood cells with high levels of CRT expression might be readily ingested by macrophages on activation compared with immature cells. The prophagocytic CRT is not expressed in HSCs; however, HSCs cannot compensate for the loss of mature cells in HLH by enhancement of hematopoiesis, because HSCs are also targeted by BM macrophages through inhibition of surface CD47 expression by inflammatory cytokines. The down-regulation of CD47 in HSCs abrogates the antiphagocytic SIRPA signal, resulting in active engulfment of HSCs by macrophages, presumably at the HSC niche. Therefore, hemophagocytosis in HLH occurs by at least 2 independent pathways mediated by CRT or CD47.

We have reported previously that in HLH patients, activated macrophages and monocytes produce a high level of cytokines such as IL-6 and TNF-α, whereas activated T cells produce IFN-γ and M-CSF.[3] These cytokines may cause the down-regulation of CD47 in HSCs that further activate macrophages. Therefore, to trigger HLH development, activation of both acquired and innate immune systems might be required. Nonetheless, our present data highlight the importance of CD47-SIRPA axis in the development of HLH, by which the HSC, the source of all blood cells, becomes the target for engulfment. Accordingly, our results suggest that the CD47-Fc protein that can bind to SIRPA on activated macrophages may be able to suppress the deregulated engulfment of HSCs in HLH. Understanding the mechanism of HSC-specific down-regulation of CD47 will be critical to the development of future therapeutic approaches for HLH.

Acknowledgments

The authors thank the Kyushu Block Red Cross Blood Center for providing umbilical cord blood samples.

This work was supported in part by a grant-in-aid from the Ministry of Education, Culture, Sports, Science and Technology in Japan (to K.A. and K.T.); a grant-in-aid from the Ministry of Health, Labor and Welfare in Japan (to K.A.); the Takeda Science Foundation (to K.T.); and the Cell Science Research Foundation (to K.T.).

Authorship

Contribution: T.K. and K.T. coordinated the project, designed and performed the experiments, analyzed the data, and wrote the manuscript; K.K., T.Y., S.D., G.Y., and Y.K. performed the experiments; J.K. analyzed the data; Y.A. and N.H. provided technical advice; and T.M., H.I., T.T., and K.A. designed the experiments, reviewed the data, and edited the manuscript.

Conflict-of-interest disclosure: The authors declare no competing financial interests.

Correspondence: Katsuto Takenaka, MD, PhD, Department of Medicine and Biosystemic Science, Kyushu University Graduate School of Medical Sciences, 3-1-1 Maidashi, Higashi-ku, Fukuoka 812-8582, Japan; e-mail: takenaka@intmed1.med.kyushu-u.ac.jp.

References

1. Janka GE. Familial and acquired hemophagocytic lymphohistiocytosis. *Eur J Pediatr.* 2007; 166(2):95-109.
2. Filipovich A, McClain K, Grom A. Histiocytic disorders: recent insights into pathophysiology and practical guidelines. *Biol Blood Marrow Transplant.* 2010;16(1 Suppl):S82-89.
3. Akashi K, Hayashi S, Gondo H, et al. Involvement of interferon-gamma and macrophage colony-stimulating factor in pathogenesis of haemophagocytic lymphohistiocytosis in adults. *Br J Haematol.* 1994;87(2):243-250.
4. Ishii E, Ohga S, Imashuku S, et al. Nationwide survey of hemophagocytic lymphohistiocytosis in Japan. *Int J Hematol.* 2007;86(1):58-65.
5. Stepp SE, Dufourcq-Lagelouse R, Le Deist F, et al. Perforin gene defects in familial hemophagocytic lymphohistiocytosis. *Science.* 1999;286(5446):1957-1959.
6. Feldmann J, Callebaut I, Raposo G, et al. Munc13-4 is essential for cytolytic granules fusion and is mutated in a form of familial hemophagocytic lymphohistiocytosis (FHL3). *Cell.* 2003; 115(4):461-473.
7. zur Stadt U, Schmidt S, Kasper B, et al. Linkage of familial hemophagocytic lymphohistiocytosis (FHL) type-4 to chromosome 6q24 and identification of mutations in syntaxin 11. *Hum Mol Genet.* 2005;14(6):827-834.
8. zur Stadt U, Rohr J, Seifert W, et al. Familial hemophagocytic lymphohistiocytosis type 5 (FHL-5) is caused by mutations in Munc18-2 and impaired binding to syntaxin 11. *Am J Hum Genet.* 2009; 85(4):482-492.
9. Bizario JC, Feldmann J, Castro FA, et al. Griscelli syndrome: characterization of a new mutation and rescue of T-cytotoxic activity by retroviral transfer of RAB27A gene. *J Clin Immunol.* 2004; 24(4):397-410.
10. Underhill DM, Ozinsky A. Phagocytosis of microbes: complexity in action. *Annu Rev Immunol.* 2002;20:825-852.
11. Greaves DR, Gordon S. Thematic review series: the immune system and atherogenesis. Recent insights into the biology of macrophage scavenger receptors. *J Lipid Res.* 2005;46(1):11-20.
12. McGreal EP, Martinez-Pomares L, Gordon S. Divergent roles for C-type lectins expressed by cells of the innate immune system. *Mol Immunol.* 2004;41(11):1109-1121.
13. Miyanishi M, Tada K, Koike M, Uchiyama Y, Kitamura T, Nagata S. Identification of Tim4 as a phosphatidylserine receptor. *Nature.* 2007; 450(7168):435-439.
14. Gardai SJ, McPhillips KA, Frasch SC, et al. Cell-surface calreticulin initiates clearance of viable or apoptotic cells through trans-activation of LRP on the phagocyte. *Cell.* 2005;123(2):321-334.
15. Orr AW, Pedraza CE, Pallero MA, et al. Low density lipoprotein receptor-related protein is a calreticulin coreceptor that signals focal adhesion disassembly. *J Cell Biol.* 2003;161(6):1179-1189.
16. Fadok VA, Bratton DL, Henson PM. Phagocyte receptors for apoptotic cells: recognition, uptake, and consequences. *J Clin Invest.* 2001;108(7): 957-962.
17. Brown EJ, Frazier WA. Integrin-associated protein (CD47) and its ligands. *Trends Cell Biol.* 2001;11(3):130-135.
18. Matozaki T, Murata Y, Okazawa H, Ohnishi H. Functions and molecular mechanisms of the CD47-SIRPalpha signalling pathway. *Trends Cell Biol.* 2009;19(2):72-80.
19. van den Berg TK, van der Schoot CE. Innate immune 'self' recognition: a role for CD47-SIRPalpha interactions in hematopoietic stem cell transplantation. *Trends Immunol.* 2008;29(5):203-206.
20. Adams S, van der Laan LJ, Vernon-Wilson E, et al. Signal-regulatory protein is selectively expressed by myeloid and neuronal cells. *J Immunol.* 1998;161(4):1853-1859.
21. Barclay AN. Signal regulatory protein alpha (SIRPalpha)/CD47 interaction and function. *Curr Opin Immunol.* 2009;21(1):47-52.
22. Oldenborg PA, Zheleznyak A, Fang YF, Lagenaur CF, Gresham HD, Lindberg FP. Role of CD47 as a marker of self on red blood cells. *Science.* 2000; 288(5473):2051-2054.
23. Blazar BR, Lindberg FP, Ingulli E, et al. CD47 (integrin-associated protein) engagement of dendritic cell and macrophage counterreceptors is required to prevent the clearance of donor lymphohematopoietic cells. *J Exp Med.* 2001;194(4): 541-549.
24. Winkler IG, Sims NA, Pettit AR, et al. Bone marrow macrophages maintain hematopoietic stem cell (HSC) niches and their depletion mobilizes HSCs. *Blood.* 2010;116(23):4815-4828.
25. Ehninger A, Trumpp A. The bone marrow stem cell niche grows up: mesenchymal stem cells and

macrophages move in. *J Exp Med.* 2011;208(3):421-428.

26. Takenaka K, Prasolava TK, Wang JC, et al. Polymorphism in Sirpa modulates engraftment of human hematopoietic stem cells. *Nat Immunol.* 2007;8(12):1313-1323.
27. Henter JI, Horne A, Arico M, et al. HLH-2004: diagnostic and therapeutic guidelines for hemophagocytic lymphohistiocytosis. *Pediatr Blood Cancer.* 2007;48(2):124-131.
28. Tsuda H. Hemophagocytic syndrome (HPS) in children and adults. *Int J Hematol.* 1997;65(3):215-226.
29. Manz MG, Miyamoto T, Akashi K, Weissman IL. Prospective isolation of human clonogenic common myeloid progenitors. *Proc Natl Acad Sci U S A.* 2002;99(18):11872-11877.
30. Mori Y, Iwasaki H, Kohno K, et al. Identification of the human eosinophil lineage-committed progenitor: revision of phenotypic definition of the human common myeloid progenitor. *J Exp Med.* 2009;206(1):183-193.
31. Fujimi A, Matsunaga T, Kobune M, et al. Ex vivo large-scale generation of human red blood cells from cord blood CD34+ cells by coculturing with macrophages. *Int J Hematol.* 2008;87(4):339-350.
32. Hashimoto S, Yamada M, Motoyoshi K, Akagawa KS. Enhancement of macrophage colony-stimulating factor-induced growth and differentiation of human monocytes by interleukin-10. *Blood.* 1997;89(1):315-321.
33. Jaiswal S, Jamieson CH, Pang WW, et al. CD47 is upregulated on circulating hematopoietic stem cells and leukemia cells to avoid phagocytosis. *Cell.* 2009;138(2):271-285.
34. Barclay AN, Hatherley D. The counterbalance theory for evolution and function of paired receptors. *Immunity.* 2008;29(5):675-678.
35. Majeti R, Chao MP, Alizadeh AA, et al. CD47 is an adverse prognostic factor and therapeutic antibody target on human acute myeloid leukemia stem cells. *Cell.* 2009;138(2):286-299.
36. Nagafuji K, Nonami A, Kumano T, et al. Perforin gene mutations in adult-onset hemophagocytic lymphohistiocytosis. *Haematologica.* 2007;92(7):978-981.
37. Chao MP, Alizadeh AA, Tang C, et al. Anti-CD47 antibody synergizes with rituximab to promote phagocytosis and eradicate non-Hodgkin lymphoma. *Cell.* 2010;142(5):699-713.
38. Chao MP, Jaiswal S, Weissman-Tsukamoto R, et al. Calreticulin is the dominant pro-phagocytic signal on multiple human cancers and is counterbalanced by CD47. *Sci Transl Med.* 2010;2(63):63ra94.
39. Maciejewski J, Selleri C, Anderson S, Young NS. Fas antigen expression on CD34+ human marrow cells is induced by interferon gamma and tumor necrosis factor alpha and potentiates cytokine-mediated hematopoietic suppression in vitro. *Blood.* 1995;85(11):3183-3190.
40. Wu HP, Chen CK, Chung K, et al. Serial cytokine levels in patients with severe sepsis. *Inflamm Res.* 2009;58(7):385-393.
41. Junker A, Krumbholz M, Eisele S, et al. MicroRNA profiling of multiple sclerosis lesions identifies modulators of the regulatory protein CD47. *Brain.* 2009;132(Pt 12):3342-3352.
42. Martins I, Kepp O, Galluzzi L, et al. Surface-exposed calreticulin in the interaction between dying cells and phagocytes. *Ann N Y Acad Sci.* 2010;1209:77-82.
43. Nagasawa T, Omatsu Y, Sugiyama T. Control of hematopoietic stem cells by the bone marrow stromal niche: the role of reticular cells. *Trends Immunol.* 2011;32(7):315-320.
44. Morrison SJ, Spradling AC. Stem cells and niches: mechanisms that promote stem cell maintenance throughout life. *Cell.* 2008;132(4):598-611.

B Cell Receptor-ERK1/2 Signal Cancels PAX5-Dependent Repression of BLIMP1 through PAX5 Phosphorylation: A Mechanism of Antigen-Triggering Plasma Cell Differentiation

Takahiko Yasuda,* Fumihiko Hayakawa,* Shingo Kurahashi,* Keiki Sugimoto,*,† Yosuke Minami,* Akihiro Tomita,* and Tomoki Naoe*

Plasma cell differentiation is initiated by Ag stimulation of BCR. Until BCR stimulation, B lymphocyte-induced maturation protein 1 (BLIMP1), a master regulator of plasma cell differentiation, is suppressed by PAX5, which is a key transcriptional repressor for maintaining B cell identity. After BCR stimulation, upregulation of BLIMP1 and subsequent suppression of PAX5 by BLIMP1 are observed and thought to be the trigger of plasma cell differentiation; however, the trigger that derepresses BLIMP1 expression is yet to be revealed. In this study, we demonstrated PAX5 phosphorylation by ERK1/2, the main component of the BCR signal. Transcriptional repression on *BLIMP1* promoter by PAX5 was canceled by PAX5 phosphorylation. BCR stimulation induced ERK1/2 activation, phosphorylation of endogenous PAX5, and upregulation of BLIMP1 mRNA expression in B cells. These phenomena were inhibited by MEK1 inhibitor or the phosphorylation-defective mutation of PAX5. These data imply that PAX5 phosphorylation by the BCR signal is the initial event in plasma cell differentiation. ***The Journal of Immunology*****, 2012, 188: 6127–6134.**

PAX5 is a member of the highly conserved paired-box (PAX) domain family of transcription factors. PAX5 is exclusively expressed from the pro-B to mature B cell stages and is downregulated during terminal differentiation into plasma cells (1). PAX5 is not only indispensable for B-lineage commitment; its continuous expression is essential for maintaining the identity of B cells (2–4). PAX5 functions as both a transcriptional activator of B lineage-specific genes and a repressor of B lineage-inappropriate genes (1) [i.e., it activates *CD19* (5), *CD79A* (6), and B cell linker protein (7) and represses CSF1 receptor (8), *Notch1* (9), and FMS-like tyrosine kinase 3 (10)]. In addition, it checks the initiation of plasma cell differentiation and the terminal differentiation of B cells by repressing B lymphocyte-induced maturation protein 1 (*BLIMP1*) and X box-binding protein 1 (11, 12).

BCR signal plays important roles in the activation, survival, and differentiation of B lymphocytes. The initial event after BCR engagement is the activation of Lyn and Syk. These kinases trigger a complex network of signaling pathways downstream of the receptor, including the Ras-Raf-MEK-ERK1/2 pathway, the Vav-cell division cycle 42-JNK pathway, and the NF-κB pathway (13). The resulting signals quickly reach the nucleus and alter gene expression. The ultimate effects on B cells are profound and vary depending on the maturation state of the cell and on additional signals that the cell receives. For germinal center B (GCB) cells, BCR signal after encountering Ag is known to initiate PAX5 downregulation, BLIMP1 upregulation, and eventually, plasma cell differentiation (14, 15). In these cells, PAX5 suppresses BLIMP1 expression and checks plasma cell differentiation. After BCR stimulation by Ag, BLIMP1 repression by PAX5 is abolished, and once BLIMP1 is expressed, it suppresses PAX5. Eventually, PAX5 is replaced by BLIMP1, which initiates plasma cell differentiation (14). The abolition of PAX5-mediated repression was thought to be the first event to initiate plasma cell differentiation (16); however, the mechanism is still unknown. In this study, we demonstrated that PAX5 was phosphorylated by ERK1/2 in vitro and in vivo at serines 189 and 283. This phosphorylation attenuated the transcriptional repression of BLIMP1 by PAX5. Finally, BCR stimulation induced the phosphorylation of ERK1/2 and PAX5, as well as BLIMP1 mRNA expression in B cells, which were inhibited by MEK1 inhibitor or the phosphorylation-defective mutation of PAX5. These data imply that PAX5 phosphorylation by the BCR signal is an initial event in plasma cell differentiation.

Materials and Methods

Cells, Abs, and reagents

Burkitt lymphoma cell line Ramos cells were cultured in RPMI 1640 medium supplemented with 10% FBS. Anti-HA Ab, anti-ERK2 Ab, and anti-PAX5 Ab (C-20) for immunoblotting, and anti-PAX5 Ab (N-19) for the supershift assay in EMSA were purchased from Santa Cruz Biotechnology (Santa Cruz, CA). Anti-human IgM Ab and anti-mouse IgM Ab for BCR stimulation and anti–phospho-ERK1/2 Ab were from Abcam (Cambridge, U.K.), Jackson ImmunoResearch Laboratories (West Grove, PA), and Cell Signaling (Beverly, MA), respectively. U0126 was obtained from Calbiochem (San Diego, CA).

Plasmids

PAX5/pCDNA, the expression vector for PAX5, was described previously (17). PAX5/pGEX and PAX5(1-279)/pGEX, expression vectors for GST-

*Department of Hematology and Oncology, Graduate School of Medicine, Nagoya University, Nagoya, 466-8550, Japan; and †Fujii Memorial Research Institute, Otsuka Pharmaceutical Co., Ltd., Otsu, 520-0106, Japan

Received for publication October 21, 2011. Accepted for publication April 17, 2012.

This work was supported by Grants-in-Aid from the National Institute of Biomedical Innovation and the Ministry of Education, Culture, Sports, Science, and Technology of Japan.

Address correspondence and reprint requests to Dr. Fumihiko Hayakawa, Department of Hematology and Oncology, Graduate School of Medicine, Nagoya University, 65 Tsurumai-cho, Showa-ku, Nagoya, 466-8550, Japan. E-mail address: bun-hy@med.nagoya-u.ac.jp

The online version of this article contains supplemental material.

Abbreviations used in this article: BLIMP1, B lymphocyte-induced maturation protein 1; GCB, germinal center B; siRNA, small interfering RNA; UTR, untranslated region.

www.jimmunol.org/cgi/doi/10.4049/jimmunol.1103039

fused full-length and partial PAX5, as well as PAX5/pBGJR, were made by subcloning PAX5 cDNA digested from PAX5/pCDNA with appropriate restriction enzymes into pGEX 5X-1 vector (Pharmacia, Uppsala, Sweden) and pBGJR, a lentivirus expression vector kindly provided by Dr. Stefano Rivella (Memorial Sloan-Kettering Cancer Center). Mutations for serine/threonine-to-alanine substitutions were introduced into PAX5/pCDNA using a QuikChange site-directed mutagenesis kit (Stratagene, La Jolla, CA). All clones were subjected to sequence analysis to confirm the introduction of the correct mutations and to exclude PCR artifacts. The expression vector for HA-tagged CA-MEK1, HA–CA-MEK1/pCMV, was described previously (18). The −1921 to +138 region (relative to the translation start site) of the *BLIMP1* promoter containing putative NF-κB- and PAX5-binding sequences was amplified by PCR, according to a previous report (19), and subcloned into pGL4.20 (Promega, Madison, WI). Two specific primer genes, 5′-TAACAGTGAGTTGATTCACTGGC-3′ (sense) and 5′-CTCGGCGGTCCCTCCTCG-3′ (antisense), were selected on the basis of the sequence of the human *BLIMP1* genomic DNA (accession number AL358952, http://www.ncbi.nlm.nih.gov/nuccore/AI358952). This reporter gene was designated as BLIMP1-luc/pGL4. Expression vectors for NF-κB p50 and p65 were purchased from Addgene (Cambridge, MA).

Transient transfection, lentivirus infection, immunoblotting, immunofluorescence, EMSA, luciferase assay, and in vitro kination assay

Transient transfection, lentivirus infection, immunoblotting, immunofluorescence, EMSA, luciferase assay, and in vitro kination assay were performed as described previously (17, 18, 20).

PAX5 knockdown

The small interfering RNA (siRNA) targeting the 5′-GACTATCCATCCATCATAA-3′ sequence in the 3′ untranslated region (UTR) of *PAX5* was purchased from Sigma-Aldrich (St. Louis, MO) and introduced into Ramos cells with nucleofector (Lonza, Wuppertal, Germany), according to the manufacturer's instructions.

Phosphate-affinity SDS-PAGE

Phosphate-affinity SDS-PAGE was performed similarly to SDS-PAGE, except that Phos-tag acrylamide-containing acrylamide gel was used. Phos-tag acrylamide was obtained from Wako Laboratory Chemicals (Osaka, Japan). In this system, Phos-tag acrylamide binds to phosphorylated amino acids during electrophoresis and slows the migration of phosphorylated proteins, according to the number of phosphorylation sites. Autoradiography or immunoblotting following electrophoresis can detect the phosphorylation of the target protein as band shifts.

Mouse spleen cell isolation

Mouse spleen cells were collected from 10-wk-old BALB/c mice and were used for immunoblotting analysis to detect PAX5 phosphorylation. Mouse spleen B cells were purified from the spleen cells using CD45R (B220) MicroBeads (Miltenyi Biotec, Bergisch Gladbach, Germany) and subjected to RT-PCR to detect BLIMP1 expression. These cells were cultured in RPMI 1640 medium supplemented with 10% FCS, 100 U/ml penicillin, and 100 U/ml streptomycin.

Real-time PCR

Total RNA was purified using the QIAamp RNA Blood Mini Kit (QIAGEN, Hilden, Germany), and reverse transcription was performed with random hexamers using the Superscript III First Strand kit (Invitrogen, Carlsbad, CA). Real-time RT-PCR was performed by standard procedures using TaqMan Universal PCR Master Mix; quantitative PCR primers for human BLIMP1 (Hs00153357), mouse Blimp1 (Mm00476128), GAPDH, or ACTB; and the ABI Prism 7000 Sequence Detection System. All of these reagents, primers, and equipment were from Applied Biosystems (Foster City, CA). Each reaction was performed in duplicate, and results were normalized by GAPDH or ACTB expression.

PAX5 DNA sequencing of clinical samples

Lymph nodes or other tissues containing tumor cells were collected with informed consent from 85 patients diagnosed with diffuse large B cell lymphoma. The sequencing study was approved by the institutional review board of Nagoya University Graduate School of Medicine. Genomic DNA was extracted from those samples with the QIAamp DNA Micro Kit (QIAGEN), according to the manufacturer's instructions. Pyrosequencing was performed for analysis of DNA mutation surrounding codons 189 and 283, according to the manufacturer's instructions. Briefly, a 125-bp sequence of exon 5, including 189 codon, or a 128-bp sequence of exon 7, including 283 codon, was amplified by PCR using biotin-tagged primers. The biotinylated PCR strands were immobilized and purified by streptavidin-Sepharose beads, denatured, and added to annealing buffer containing 250 nM sequencing primer. Sequencing was carried out with the PyroMark Q96 ID system (QIAGEN). DNA sequences corresponding to codons 181–199 and codons 273–292 were analyzed using two sequence primers. Primers used in this analysis are described in Supplemental Table I.

Results

PAX5 is phosphorylated by ERK2 in vitro

It was recently reported that ERK1/2 signal was a key initiation signal for BLIMP1 expression and plasma cell differentiation of GCB cells (21); however, the detailed mechanism of ERK1/2 signal that induces BLIMP1 expression is still unknown. Combined with the open question about the initial event in plasma cell differentiation, these findings gave rise to the speculation that PAX5 phosphorylation by ERK1/2 negatively affected BLIMP1 repression by PAX5 and is the trigger of plasma cell differentiation. To test whether PAX5 can be phosphorylated in response to ERK1/2 signal, we performed an in vitro kinase assay using GST-PAX5 as a substrate. rERK2 efficiently phosphorylated full-length PAX5 and the N-terminal region of PAX5, whereas JNK did not (Supplemental Fig. 1A). Inspection of the PAX5 sequence revealed the presence of eight ERK1/2 consensus sites, S/T-P. Therefore, we introduced a series of alanine substitutions at these sites to map the actual phosphorylation sites by ERK2 and to check the phosphorylation status with the phosphate-affinity SDS-PAGE system. In this system, PAX5 phosphorylation by ERK2 was detected as two shifted bands (Fig. 1A), suggesting that PAX5 had two phosphorylation sites. Substitutions of alanine at codons 189, 283, and 285 (combined mutation), as well as at 283, caused the disappearance of one of the shifted bands, whereas other substitutions, including at codon 285, did not affect the shifted bands (Fig. 1A, Supplemental Fig. 1B, 1C), indicating that the phosphorylation sites were serines 189 and 283. Consistently, all shifted bands disappeared by combined substitution at codons 189 and 283 (Fig. 1A).

PAX5 phosphorylation occurred in vivo through ERK1/2 signaling

We next examined whether PAX5 phosphorylation occurred by the activation of ERK1/2 in vivo. Coexpression of the constitutively active mutant of MEK1 (CA-MEK1, an upstream activator of endogenous ERK1/2) in 293T cells caused similar PAX5 phosphorylation as in vitro (i.e., two shifted bands were observed in phosphate-affinity SDS-PAGE and disappeared by the mutation at ERK2 phosphorylation sites determined in vitro) (Fig. 1B). These results indicated that ERK1/2 could also phosphorylate PAX5 in vivo. We demonstrated the schema of the PAX5 structure, pointing out the phosphorylation sites. The amino acid sequences surrounding the phosphorylation sites are conserved evolutionarily, except in zebrafish (Fig. 1C).

Next, we attempted to determine whether endogenous PAX5 was phosphorylated by BCR stimulation. We stimulated BCR by anti-IgM Ab in Ramos cells, a cell line of Burkitt lymphoma, which is thought to be a tumor of GCB cells. Strikingly, BCR stimulation induced strong ERK1/2 phosphorylation and PAX5 phosphorylation in Ramos cells. This phosphorylation was inhibited by the MEK1 inhibitor, U0126, indicating the mediation of PAX5 phosphorylation by ERK1/2 signal (Fig. 2A). Furthermore, to examine whether BCR signal-induced PAX5 phosphorylation

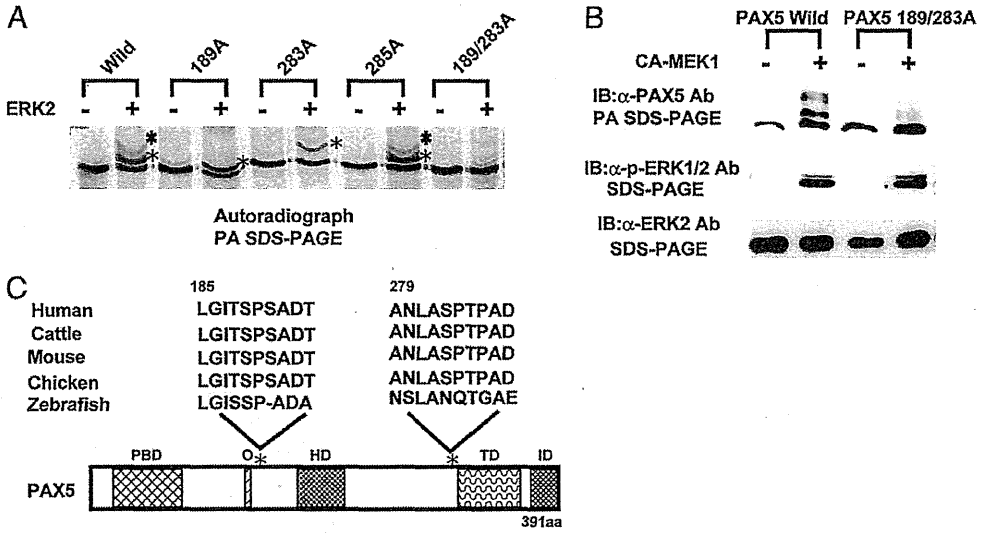

FIGURE 1. PAX5 was phosphorylated by ERK1/2 signal. (**A**) PAX5 was phosphorylated by ERK2 at serines 189 and 283 in vitro. Wild-type PAX5 and PAX5 with the indicated mutations were synthesized in vitro with [^{35}S]-labeling. Mutations are designated by the codon number followed by "A". PAX5 proteins were phosphorylated in vitro with ERK2 and were separated by phosphate-affinity (PA) SDS-PAGE, in which phosphorylated proteins migrate slowly relative to the number of phosphorylation sites. The regular asterisks and bold asterisks indicate PAX5 phosphorylated at one site and two sites, respectively. Mutants of 189A and 283A showed only one shifted band, and all shifted bands disappeared by the mutation of 189/283A, suggesting that serines 189 and 283 were the phosphorylation sites. (**B**) PAX5 was phosphorylated by ERK1/2 in vivo. 293T cells (1×10^5) were transfected with wild-type or mutant PAX5 expression vector (200 ng), with or without cotransfection of constitutively active MEK1 (CA-MEK1) expression vector (200 ng). Cell lysates were separated by PA SDS-PAGE or SDS-PAGE, as indicated, and subjected to immunoblotting (IB). Wild-type PAX5 was phosphorylated by the coexpression of CA-MEK1, but mutant PAX5 was not. (**C**) Conservation of PAX5 phosphorylation sites beyond species. Alignment of amino acid sequences of human, cattle, mouse, chicken, and zebrafish PAX5 corresponding to the phosphorylation sites of human PAX5. Asterisks indicate phosphorylation sites of human PAX5. Amino acid sequences surrounding PAX5 phosphorylation sites are completely conserved, except in zebrafish. HD, Homeobox domain; ID, inhibitory domain; O, conserved octapeptide; PBD, paired box domain; TD, transactivation domain.

occurred at ERK2 phosphorylation sites determined in vitro, we established stable Ramos transfectants of control vector and the expression vectors of wild-type and phosphorylation-defective mutant of PAX5, designated as Control-Ramos, PAX5 Wild-Ramos, and PAX5 189/283A-Ramos, respectively. Because phosphorylation of endogenous PAX5 masked the difference in the phosphorylation status between exogenously expressed wild-type and mutant PAX5 (data not shown), we further introduced the siRNA targeting 3′ UTR of endogenous PAX5 to specifically knockdown endogenous PAX5 of these transfectants. Successful specific knockdown of endogenous PAX5 is demonstrated in Fig. 2B. In this system, BCR signal-induced PAX5 phosphorylation was completely diminished by the mutation at ERK2 phosphorylation sites (Fig. 2C). These results indicated that BCR signal-induced PAX5 phosphorylation was mediated by ERK1/2.

We also performed the same experiment in Fig. 2A using mouse spleen cells that were rich in primary B cells. The results were similar to that in Ramos cells. BCR stimulation of mouse spleen cells induced ERK1/2 phosphorylation and PAX5 phosphorylation, which was inhibited by U0126 (Fig. 2D). These results suggested that PAX5 phosphorylation by ERK1/2 in response to BCR stimulation also occurred in primary normal B cells.

ERK1/2 signal canceled PAX5-dependent transcriptional repression of BLIMP1

Next, we set out to identify the effect of phosphorylation on BLIMP1 repression by PAX5. To replicate BLIMP1 repression by PAX5 in the luciferase assay, we constructed a reporter gene containing an ~2-kbp region of *BLIMP1* promoter, including putative binding sites for PAX5, and NF-κB, one of the BLIMP1 expression activators, according to a previous report (19) (Fig. 3A). Before the assay, we focused on enhancement of PAX5 expression by CA-MEK1 coexpression observed in Fig. 1B, because it may affect the luciferase assay comparing PAX5 function with and without CA-MEK1 coexpression. We judged that this enhancement of PAX5 expression is due to a nonspecific effect of ERK1/2 signal on the transcriptional machinery on the T7 or CMV promoter of PAX5/pCDNA, because CA-MEK1 coexpression also enhanced the expression of the phosphorylation-defective mutant of PAX5 (Fig. 1B), indicating that this phenomenon was independent of PAX5 phosphorylation, and BCR stimulation or CA-MEK1 expression in Ramos cells did not affect the expression level of endogenous PAX5 (Fig. 2A, data not shown). Therefore, we investigated the effect of CA-MEK1 coexpression on PAX5 expression in detail (Supplemental Fig. 2A) and adjusted the amount of PAX5 expression vector used for the luciferase assay when it was cotransfected with the CA-MEK1 expression vector to keep the PAX5 expression level constant. A constant expression of PAX5 among luciferase samples was confirmed by immunoblotting (Fig. 3B, *lower panel*).

Luciferase expression was strongly induced by NF-κB expression, which was decreased to 15% of the control level by wild-type PAX5 coexpression (Fig. 3B, *lane 2* versus *lane 4*). Importantly, CA-MEK1 coexpression increased the luciferase expression suppressed by wild-type PAX5 to 80% of the control level (Fig. 3B, *lane 3* versus *lane 5*), indicating that ERK1/2 signal canceled transcriptional repression by PAX5. Furthermore, transcriptional repression by mutant PAX5 was attenuated by CA-MEK1 coexpression to a significantly lesser extent than that by wild-type PAX5 (Fig. 3B, *lane 5* versus *lane 7*, $p < 0.05$), indicating its resistance to ERK1/2 signal-dependent cancellation of the transcriptional repression. These data suggested that PAX5 phosphorylation by ERK1/2 signal played an important role in the abolition of BLIMP1 repression by PAX5.

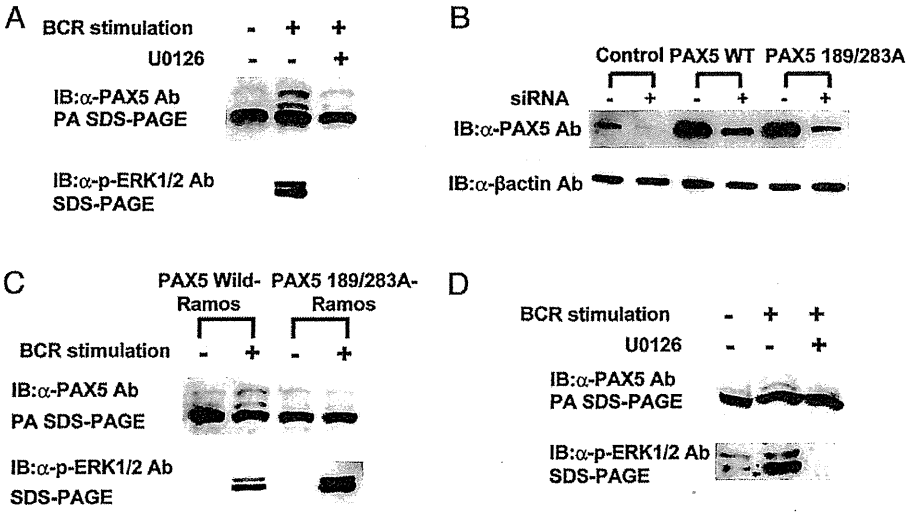

FIGURE 2. PAX5 phosphorylation was induced by BCR stimulation through ERK1/2 signal in B cells. (**A**) MEK1 inhibitor inhibited BCR signal-induced PAX5 phosphorylation. Ramos cells were stimulated with anti-IgM Ab (2 μg/ml) for 10 min. U0126 (10 μM) was added 60 min before stimulation, as indicated. Cell lysates were subjected to immunoblotting analyses, as in Fig. 1B. PAX5 phosphorylation was induced by BCR stimulation, which was inhibited by U0126. (**B**) Specific knockdown of endogenous PAX5 in Ramos cells. The indicated PAX5 stable transfectants of Ramos cells were introduced control siRNA (−) and siRNA targeting the 3′-UTR of endogenous PAX5 (+), as indicated. Twenty-four hours later, cells were lysed and subjected to immunoblotting. Reduction of PAX5 expression by siRNA introduction was much stronger in Control-Ramos cells that expressed only endogenous PAX5 than in PAX5 Wild-Ramos cells and PAX5 189/283A-Ramos cells that expressed endogenous and exogenous PAX5, indicating specific knockdown of endogenous PAX5. (**C**) The mutations at ERK2 phosphorylation sites abolished BCR signal-induced PAX5 phosphorylation. The siRNA targeting the 3′-UTR of endogenous PAX5 mRNA was introduced into PAX5 Wild-Ramos cells and PAX5 189/283A-Ramos cells to knockdown endogenous PAX5 specifically. Then, cells were stimulated with anti-IgM Ab, lysed, and subjected to immunoblotting analyses, as in (A). (**D**) MEK1 inhibitor inhibited BCR signal-induced PAX5 phosphorylation in mouse spleen cells. Mouse spleen cells were treated and analyzed as in (A), except that cells were stimulated with anti-IgM Ab (10 μg/ml) for 10 min.

Of note, mutant PAX5 suppressed the luciferase expression more strongly than did wild-type PAX5 when CA-MEK1 was not coexpressed (Fig. 3B, *lane 4* versus *lane 6*). This is probably due to mild attenuation of wild-type PAX5 ability by weak phosphorylation of PAX5 by constitutively activated ERK1/2 signal in 293T cells, because ERK1/2 was weakly, but constitutively, phosphorylated in 293T cells without CA-MEK1 coexpression (Supplemental Fig. 2B), and administration of U0126 enhanced

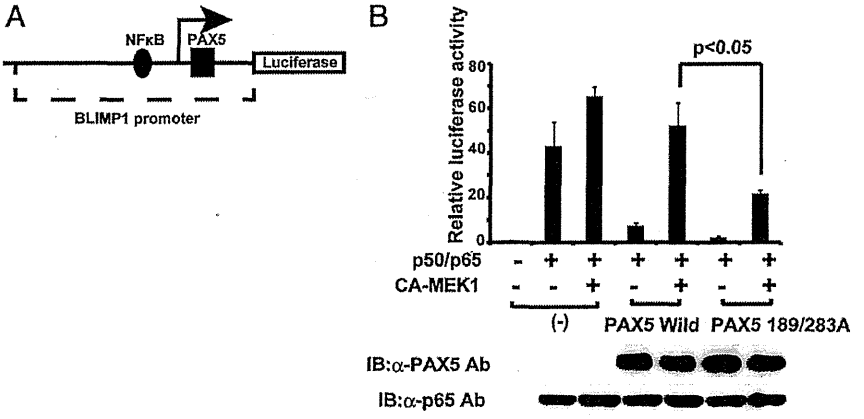

FIGURE 3. PAX5 phosphorylation attenuates transcriptional repression by PAX5. (**A**) Schematic representation of BLIMP1-luc/pGL4, the reporter plasmid for analysis of transcriptional repression by PAX5. The part of the *BLIMP1* promoter (~2 kbp) containing putative NF-κB– and PAX5-binding sequences was subcloned to luciferase reporter plasmid. (**B**) Transcriptional repression by PAX5. Luciferase assay was performed using BLIMP1-luc/pGL4. When CA-MEK1 expression vector was cotransfected, the amount of PAX5 expression vectors was reduced from 100 to 20 ng to avoid elevation of the PAX5 expression level by CA-MEK1 coexpression. Triplicate sets of cells were lysed separately: two sets for the luciferase assay using luciferase assay buffer and the other set for immunoblotting using whole-cell extraction buffer. Luciferase activities in three independent transfection experiments are shown as average values relative to the basal activity observed in control cells (results are the mean ± SD). Cell lysates were also subjected to immunoblotting (IB), as indicated, to confirm the equal expressions of PAX5 (*middle panel*). The expression vectors of NF-κB p50 and p65 were 50 ng each and were not adjusted in cotransfection with CA-MEK1. Equal expressions of NF-κB p65 were also confirmed by immunoblotting (*bottom panel*). Statistical comparisons were performed using the *t* test. Wild-type and mutant PAX5 suppressed NF-κB–induced luciferase expression. Transcriptional repression by wild-type PAX5 was canceled by CA-MEK1 coexpression, whereas that by mutant PAX5 was significantly more resistant to CA-MEK1 coexpression (*lane 5* versus *lane 7*, $p < 0.05$).